

# Quantitative Characterization of Dispersed Particle Size, Size Distribution, and Matrix Ligament Thickness in Polypropylene Blended with Metallocene Ethylene–Octene Copolymers

K. PREMPHET, W. PAECHAROENCHAI

Department of Chemistry, Mahidol University, Rama VI Road, Bangkok 10400, Thailand

Received 21 November 2000; accepted 22 December 2000

**ABSTRACT:** The average rubber particle size, size distribution, and matrix ligament thickness between particles in polypropylene blends containing metallocene catalyzed ethylene–octene copolymers have been quantitatively analyzed, as functions of blend composition and phase viscosity ratio. Comparison has been made between experimental data and those predicted from a number of theoretical models. All blends showed two-phase morphology, with interestingly a bimodal distribution of the rubber particle size. The ranges and averages of rubber particle size were mainly determined by blend composition and viscosity ratio between the phases, irrespective of comonomer content along the rubber chains. The logarithmic relationship between the matrix ligament thickness and rubber concentration was observed. The values of ligament thickness obtained from the experiments and theoretical models were not in agreement. © 2001 John Wiley & Sons, Inc. *J Appl Polym Sci* 82: 2140–2149, 2001

**Key words:** particle size; size distribution; ligament thickness; polypropylene blends; ethylene–octene copolymers

## INTRODUCTION

Polypropylene (PP), although it has been extensively used for many applications, possesses low-temperature impact strength. It is well known that the impact properties of polypropylene can be considerably enhanced by the incorporation of a rubbery material such as the ethylene–propylene copolymer,<sup>1,2</sup> ethylene–propylene diene terpolymer,<sup>3,4</sup> and ethylene–octene copolymer.<sup>5,6</sup> During mixing, discrete rubber particles are formed and randomly dispersed in the polymer matrix. These rubber particles act as stress concentrators, promoting crazing, and/or shear yield-

ing of the polymer matrix. In polymer/polymer blends, the important morphological parameters include the average rubber particle size and size distribution, interparticle distance (matrix ligament thickness), and spatial distribution of rubber particles in the polymer matrix.

Wu<sup>7</sup> proposed that the matrix ligament thickness is the only parameter that determines whether a blend will be tough or brittle. A blend will be tough if the matrix ligament thickness is smaller than the critical value. For the cubic packing of spherical particles with uniform size, the matrix ligament thickness ( $T$ ) can be obtained from eq. (1)

$$T = d[(\pi/6\phi)^{1/3} - 1] \quad (1)$$

Correspondence to: K. Premphet.

*Journal of Applied Polymer Science*, Vol. 82, 2140–2149 (2001)  
© 2001 John Wiley & Sons, Inc.

where  $d$  is the rubber particle diameter and  $\phi$  is the rubber volume fraction. The  $T$  value was found to be dependent on the matrix characteristics,<sup>8,9</sup> properties of the rubber phase,<sup>10,11</sup> strain rate,<sup>12</sup> etc. The critical matrix ligament thickness has been found in several rubber-toughened polymers, such as nylon,<sup>7,8</sup> polypropylene,<sup>13</sup> and polyvinyl chloride.<sup>14–19</sup>

To account for the effect of particle size distribution ( $\sigma$ ), eq. (1) was modified and the following equation was obtained.<sup>8</sup>

$$T = d[(\pi/6\phi)^{1/3} - 1]\exp(\ln^2\sigma) \quad (2)$$

Equation (3) was derived by Liu et al.<sup>14</sup> for calculating matrix ligament thickness of polymer blends with a morphology of well-dispersed particles as follows:

$$T = d[(\pi/6\phi)^{1/3}\exp(1.5 \ln^2\sigma) - \exp(0.5 \ln^2\sigma)] \quad (3)$$

The particle size distribution parameter ( $\sigma$ ) can be calculated from eq. (4).

$$\ln \sigma = \sqrt{\frac{\sum_{i=1}^N n_i (\ln d_i - \ln d)^2}{\sum_{i=1}^N n_i}} \quad (4)$$

In the case of monodispersity, the value of  $\sigma$  is equal to 1; and when there is polydispersity,  $\sigma$  is greater than 1.

In addition to the average particle size, size distribution, and the interparticle distance, the particle spatial distribution (spatial packing or dispersion state) is another morphological parameter that has been reported to influence the brittle–ductile transition of polymer blends.<sup>17–19</sup> To obtain a toughened blend, the morphology of well-dispersed particles is usually expected. However, there is another spatial distribution that was reported to give a much higher toughening efficiency than the morphology of well-dispersed particles,<sup>20–23</sup> which has been called the pseudonetwork morphology.<sup>17–20</sup> The relationship between rubber spatial distribution ( $\xi$ ) and other morphological parameters is shown in eq. (5).

$$T = d[\xi(\pi/6\phi)^{1/3}\exp(1.5 \ln^2\sigma) - \exp(0.5 \ln^2\sigma)] \quad (5)$$

For polymer blends with the morphology of well-dispersed particles,  $\xi$  is equal to 1; and for the pseudonetwork morphology,  $\xi$  is smaller than 1.

The present article aims to report the effects of blend composition and phase viscosity ratio on the morphology of polypropylene (PP) and ethylene–octene copolymer (EORs) blends. The average rubber particle size, size distribution, and matrix ligament thickness between rubber particles were quantitatively analyzed and compared to those predicted from theoretical models. The correlation between blend morphology and mechanical properties will subsequently be reported.

## EXPERIMENTAL

### Materials

The polymers used in this study were an isotactic polypropylene (PP) (P400S) supplied by Thai Polyethylene Co. Ltd., Thailand; and three metallocene catalyzed ethylene–octene copolymers (EOR) (ENGAGE 8150, ENGAGE 8200, ENGAGE 8003) supplied by DuPont Dow Elastomer Co. The molecular characteristics of these polymers are shown in Table I. The rheological properties of PP and EORs were studied using a Rosand RH-2000 capillary rheometer. Figure 1 shows the plot of log viscosity against log shear rate for PP and EORs.

### Blending and Sample Preparation

The PP and EOR copolymers were melt-mixed in an intermeshing corotating twin screw extruder (PRISM TSE 16). The temperature profile was controlled at 160, 180, 185, 200, and 200°C from feed to die zones. The screw speed was kept constant at 150 rpm. The concentrations of EOR in the blends were varied in the range of 0–30% vol, because at a higher concentration of EOR (i.e., 40%), coalescence of the dispersed EOR particles became predominant. This added more complications to the morphological analysis. In this study, all blends were prepared under the same processing conditions.

### Phase Morphology Studies

SEM was used to examine the phase morphology of the blends. The samples were cryogenic fractured and etched with heptane vapor for 20 s to remove the EOR particles, thus improving con-

**Table I** Material Characteristics

Properties	Materials			
	PP	EOR1	EOR2	EOR3
Trade name	P400S	E8150	E8003	E8200
Melt flow index (g/10 min)	3.5	0.5	1.0	5.0
Density (g/cm <sup>3</sup> )	0.903	0.868	0.885	0.87
Mooney viscosity (ML 1+4 @ 121°C)	—	35	22	8
Octene content (% mol) <sup>a</sup>	—	10.9	7.6	10.0
Molecular weight (g/mol) <sup>b</sup>	458,385	213,110	151,139	111,056
Molecular weight distribution	5.91	2.5	2.3	3.01

<sup>a</sup> Determined by <sup>13</sup>C NMR.<sup>b</sup> Determined by GPC.

trast between the two phases. The specimens were then sputter coated with platinum-palladium prior to SEM examination. An Hitachi S2500 scanning electron microscope operating at 15 kV was used to view the specimens. The SEM micrographs were then used to analyze the rubber particle size and shape, size distribution, and the distances between particles (ligament thickness). The analysis was carried out using a computerized image analyzer with Image-Pro Plus software. Typically, 400–700 particles and several fields of view were measured. The number ( $d_n$ ), weight ( $d_w$ ), and volume ( $d_v$ ) average rubber particle sizes in the blends were calculated using the following equations.<sup>24, 25</sup>

$$d_n = \frac{\sum_{i=1}^N n_i d_i}{\sum_{i=1}^N n_i} \quad (6)$$

$$d_w = \frac{\sum_{i=1}^N n_i d_i^2}{\sum_{i=1}^N n_i d_i} \quad (7)$$

$$d_v = \frac{\sum_{i=1}^N n_i d_i^4}{\sum_{i=1}^N n_i d_i^3} \quad (8)$$

where  $n_i$  is the number of rubber particles within the diameter range  $i$ . For the ligament thickness, the surface-to-surface distances between neighboring rubber particles were measured.

## RESULTS AND DISCUSSION

### Dispersed Particle Size

Figures 2–4 show cryogenic fractured and etched surfaces of PP/EOR1, PP/EOR2, and PP/EOR3 blends, respectively. The rubber phase appears as dark circular holes within the PP matrix. The two

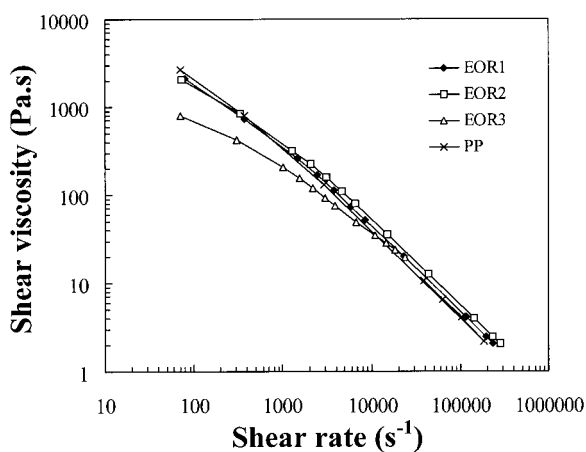


**Figure 1** Log shear viscosity against log shear rate for PP and EORs.

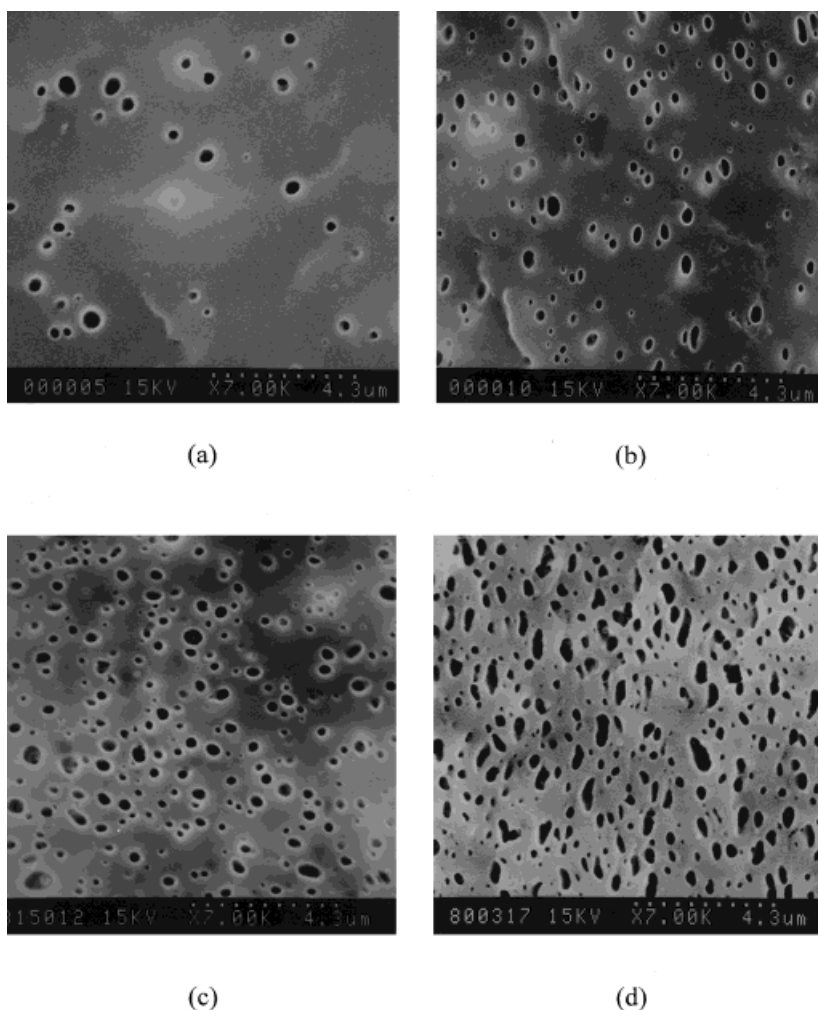


**Figure 2** Cryogenic fractured and etched surfaces of PP/EOR1 blends: (a) 5, (b) 10, (c) 20, and (d) 30% vol of EOR.

phase morphology is clearly visible at all compositions. The amount of discrete rubber particles evidently increases with increasing rubber concentration. Visual inspection of SEM micrographs suggested that the size and shape of the dispersed particles are similar in the blends containing EOR up to 20%. The distribution of the rubber particle size seems to become broader as the content of EOR in the blends increases. Generally, a uniform distribution of the minor phase will be obtained when the mixed polymers have similar melt viscosities, no matter which is the minor component.<sup>26,27</sup> In the case where the components have different viscosities, the morphology of the resultant blend depends on whether the minor component has a lower or higher viscosity than that of the major one. If the minor component has a lower viscosity, the minor component will be

finely dispersed. On the other hand, the minor component will be coarsely dispersed if its viscosity is higher than that of the major one. However, there were some contradictory results reported in the literature.<sup>28</sup>

To provide a quantitative assessment of composition effect on rubber dispersion, representative rubber particles were measured and counted using an image analyzer. The number ( $d_n$ ), weight ( $d_w$ ), and volume ( $d_v$ ) average rubber particle sizes as well as the most frequently occurring sizes ( $d_1$  and  $d_2$ ) of various blends are shown in Table II. For a given rubber system at low rubber concentrations (0–10 vol %), the average dispersed phase sizes change slightly with composition. In the strong shear field developed during intense melt mixing and for low rubber concentrations, the extent of dispersion and the proba-

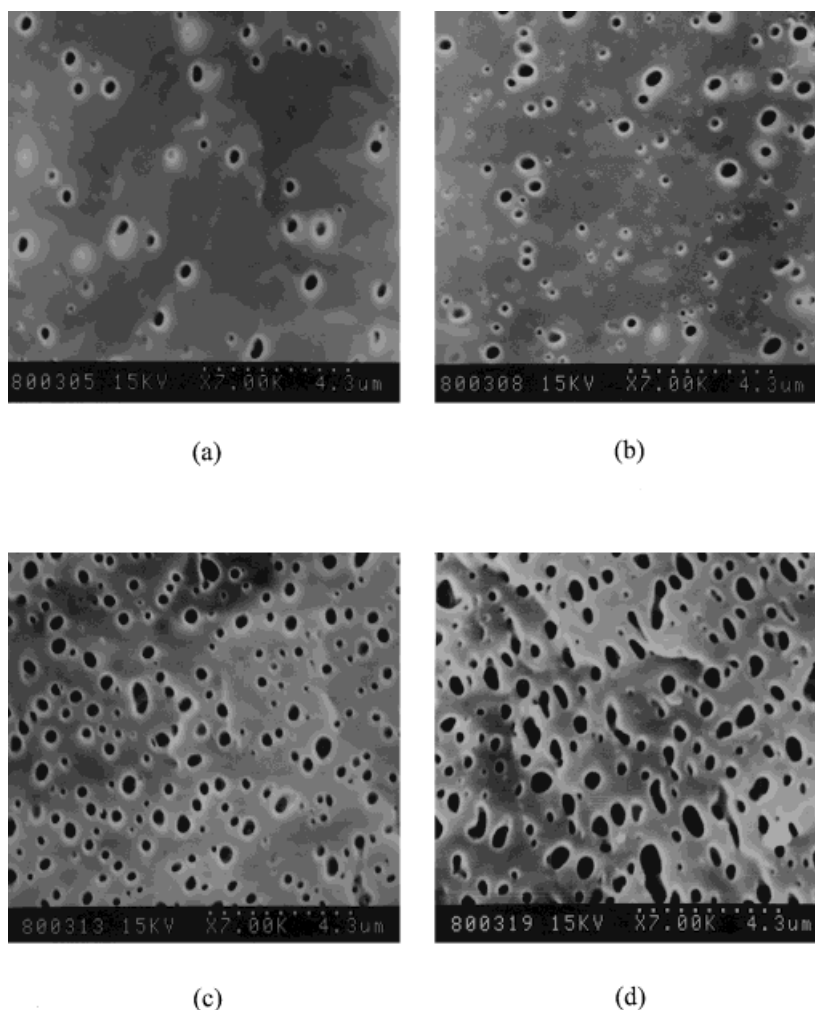


**Figure 3** Cryogenic fractured and etched surfaces of PP/EOR2 blends: (a) 5, (b) 10, (c) 20, and (d) 30% vol of EOR.

bility of particle recombination probably remains independent of composition. Increasing rubber concentration further to 30 vol %, an increase in average rubber particle size is observed. This is believed to be due to the presence of populations of larger sizes in the system. The majority of the rubber particles, however, still have the same sizes, which can be clearly seen from the histograms of Figure 5. In the present study, all blends interestingly show a bimodal distribution of the rubber particle sizes at  $d_1$  of 0.1  $\mu\text{m}$  and  $d_2$  of 0.3  $\mu\text{m}$ . With increasing the rubber content in the blends, the particle size at bimodal distribution peaks ( $d_1$  and  $d_2$ ) remained constant (Table II). Varying the EOR used shows no influence on these values.

To study the effect of phase viscosity ratio on the blend morphology, the comparison of the av-

erage particle sizes was made between the blends of EOR1, EOR2, and EOR3. In the range of shear rate developed during mixing in the extruder ( $\sim 600 \text{ s}^{-1}$ ), the viscosities of EOR1 and EOR2 are very similar to that of PP ( $\eta_d/\eta_m = 1$ ), whereas the viscosity of EOR3 is considerably lower ( $\eta_d/\eta_m = 0.5$ ) (Fig. 1). From Table II, it can be seen that the average phase sizes ( $d_n$ ,  $d_w$ , and  $d_v$ ) of PP/EOR1 and PP/EOR2 blends were rather similar and slightly larger than those of PP/EOR3 blends, especially at high concentration of EOR. The range of particle size and the average particle size of the dispersed rubber phase were found to be determined mainly by the value of phase viscosity ratio and composition, irrespective of comonomer content along the EOR chain. Under the same processing conditions, the EOR3 with its relatively low viscosity had a strong tendency toward



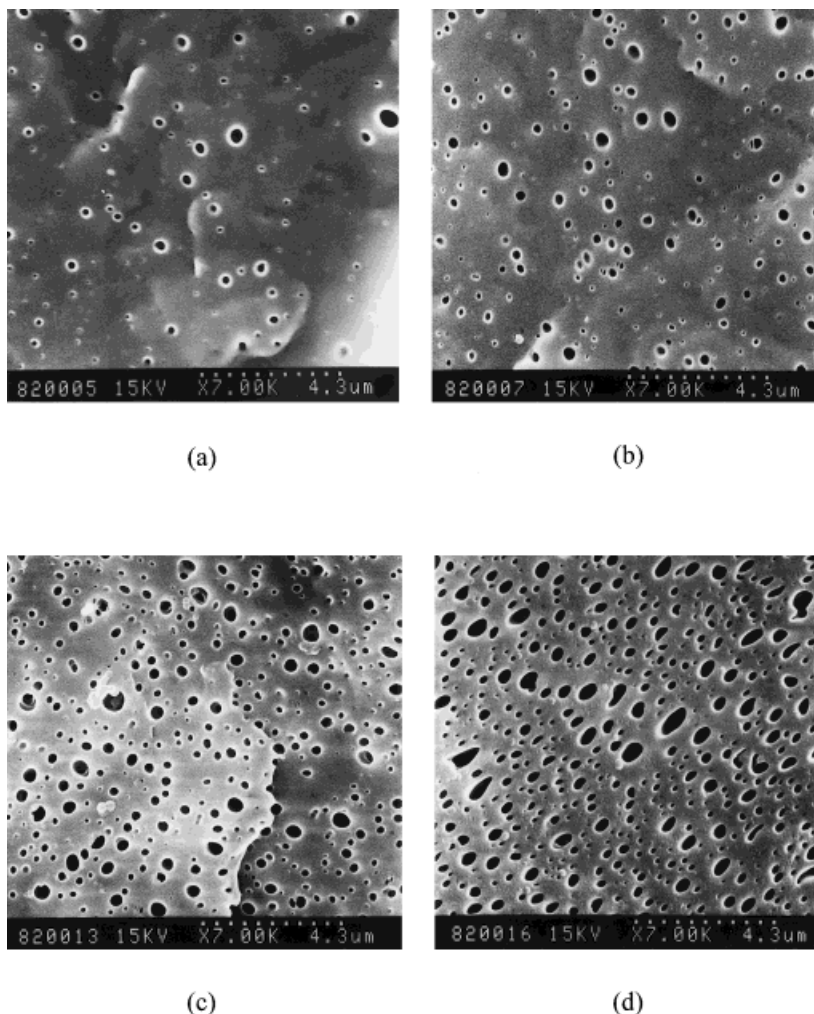


**Figure 4** Cryogenic fractured and etched surfaces of PP/EOR3 blends: (a) 5, (b) 10, (c) 20, and (d) 30% vol of EOR.

droplet breakup, and thus the coalescence probability at high rubber loading was reduced compared to EOR1 and EOR2. The type of dependence of the size of the dispersed particles upon the phase viscosity ratio observed for the PP/EOR systems investigated agrees well with those found for PP/EPDM,<sup>29</sup> PP/EPR,<sup>30</sup> and PP/PC<sup>31</sup> blends.

#### Particle Size Distribution

To evaluate the dispersity of rubber particle size in the blends, the particle size distribution parameter ( $\sigma$ ) may be calculated either by using eq. (4) or from the log-normal distribution plot of the cumulative number densities of particles at or below a specific size against particle diameter.<sup>14</sup> A Gaussian distribution of particles would appear

as a straight line with the number average particle size at 50% and the standard deviation inversely proportional to the slope. A steep slope indicates a narrow distribution. A monodisperse distribution would be a vertical line. Curvature indicates deviation from the Gaussian form and generally reflects skewness in the distribution. A bimodal distribution would appear as two straight line regions, if both populations are Gaussian. The offset and slopes are the means and standard deviations of the two populations.<sup>28</sup> In the present blends, cumulative distribution plot of Figure 6 appears as two straight lines, indicating a bimodality of rubber particle size. The bimodal distribution of rubber particles in the present study can also be clearly observed from the histograms of Figure 5. Generally, uni-

**Table II** The Number ( $d_n$ ), Weight ( $d_w$ ), and Volume ( $d_v$ ) Average Rubber Particle Sizes, the Frequent Occurring Sizes ( $d_1$ ,  $d_2$ ), and the Particle Size Distribution Parameter ( $\sigma$ ) of Various Blends

Blend	% Vol of Rubber	Size Range ( $\mu\text{m}$ )	Average Particle Size ( $\mu\text{m}$ )			Frequent Occurring Size ( $\mu\text{m}$ )		$\sigma$
			$d_n$	$d_w$	$d_v$	$d_1$	$d_2$	
PP/EOR1 ( $\eta_d/\eta_m = 0.9$ )	5	0.10–0.55	0.20 (0.11) <sup>a</sup>	0.27 (0.11)	0.40 (0.11)	0.15	0.33	1.51
	10	0.08–0.55	0.18 (0.10)	0.24 (0.10)	0.37 (0.10)	0.10	0.33	1.58
	20	0.08–0.60	0.19 (0.11)	0.26 (0.11)	0.38 (0.11)	0.10	0.30	1.68
	30	0.08–0.75	0.26 (0.15)	0.35 (0.15)	0.46 (0.15)	0.10	0.33	1.92
PP/EOR2 ( $\eta_d/\eta_m = 1.0$ )	5	0.08–0.48	0.18 (0.10)	0.24 (0.10)	0.33 (0.10)	0.10	0.33	1.63
	10	0.08–0.53	0.17 (0.10)	0.22 (0.10)	0.35 (0.10)	0.10	0.30	1.65
	20	0.08–0.70	0.25 (0.14)	0.33 (0.14)	0.44 (0.14)	0.10	0.30	1.88
	30	0.08–0.83	0.28 (0.17)	0.38 (0.17)	0.51 (0.17)	0.10	0.30	1.95
PP/EOR3 ( $\eta_d/\eta_m = 0.5$ )	5	0.08–0.35	0.10 (0.04)	0.11 (0.04)	0.12 (0.04)	0.10	0.30	1.28
	10	0.08–0.38	0.13 (0.06)	0.16 (0.06)	0.24 (0.06)	0.10	0.30	1.40
	20	0.08–0.57	0.19 (0.14)	0.27 (0.14)	0.42 (0.14)	0.10	0.30	1.84
	30	0.08–0.60	0.18 (0.12)	0.26 (0.12)	0.39 (0.12)	0.10	0.30	1.77

<sup>a</sup> Standard deviation in parentheses.

modal distribution was observed in most polymer blends such as nylon 66/EPR,<sup>7</sup> nylon 6/ULDPE,<sup>32</sup> and PP/EPDM blends.<sup>33</sup> However, Jang observed a bimodal distribution of SBR particles in PP/SBR blends.<sup>29</sup> The occurrence of bimodal distribution of the rubber particles in the studied blends is unclear at present.

To calculate the  $\sigma$  parameter from the log-normal distribution plot, the curve must be perfectly fit as a straight line. Unfortunately, the curves of the present study deviated from the log-normal distribution due to the bimodality of sizes. Therefore, particle size parameter is calculated from eq. (4), and is shown in Table II. The  $\sigma$  values of PP/EOR blends range from 1.28 to 1.95, indicating polydispersity in these blends. The polydispersity of the particle size distribution is found to increase with increasing the rubber concentration.

### Matrix Ligament Thickness

Another important parameter that has a strong effect on toughness of binary polymer blends is the matrix ligament thickness. The matrix ligament thickness was defined by Wu as the surface to surface distances between rubber particles in the matrix.<sup>8</sup> It may be obtained by either experimental measurement or calculating from various theoretical equations. In this work, the values of matrix ligament thickness ( $T$ ) were measured and compared with those calculated from eqs. (1)–(3). In the calculation of  $T$ , the  $\sigma$  values calculated from eq. (4) were used. Figure 7 shows the logarithmic relationship between the matrix ligament thickness ( $T$ ) and rubber concentration. An increase in rubber concentration led to a decrease in the  $T$  values. This is as expected, because there were a larger amount of rubber particles dispersed in the blends. At low rubber concentra-

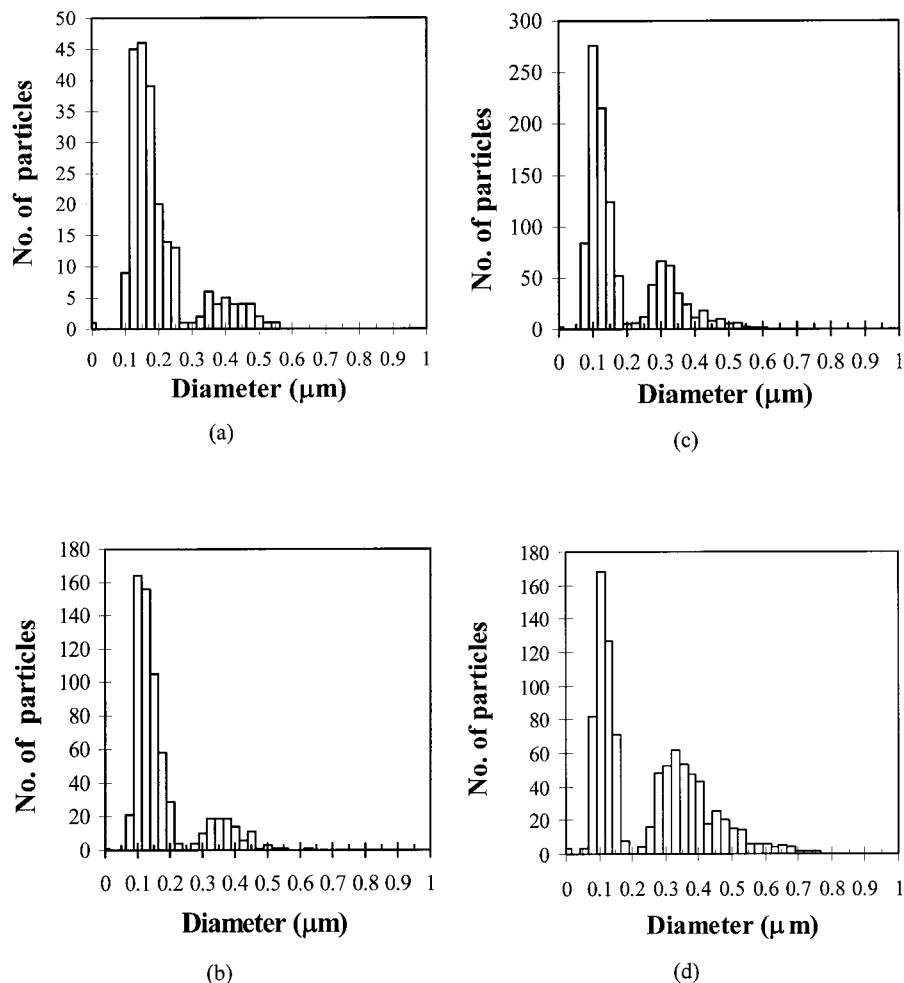


**Figure 5** Histograms of rubber particle sizes in PP/EOR1 blends: (a) 5, (b) 10, (c) 20, and (d) 30% vol of EOR.

tions (<20 vol %), the greatest ligament thickness was found in the PP/EOR1 blends, whereas the lowest were observed in the PP/EOR3 systems. The differences in matrix ligament thickness can be negligible when the concentration of EOR is higher than 20 vol %. The comparison of  $T$  values obtained from the experimental measurement and the theoretical calculations for PP/EOR1 blends is demonstrated in Figure 8. It can be seen that the experimental  $T$  values did not fit the theoretical calculations. This may be partly due to a complication in the blend morphology where two populations of particle sizes existed. The similar observations were also found for the blends of PP/EOR2 and PP/EOR3.

## CONCLUSIONS

Quantitative characterization of dispersed particle size, size distribution, and matrix ligament

thickness in PP/EOR blends was carried out. SEM study revealed a two-phase morphology where EOR as droplets dispersed in the PP matrix. Cumulative log-normal distribution plots showed two populations of particle size in the blends. The occurrence of bimodal distribution was unclear at present. For the blend systems with low rubber content, the average rubber particle sizes slightly increased with composition. A further increase in rubber content contributes to an increase in average particle sizes caused by the presence of populations of larger sizes in the system. The matrix ligament thickness ( $T$ ) was found to be related to rubber concentration in a logarithmic relation. A decrease in the  $T$  values was found when the rubber concentration increased and the phase viscosity ratio decreased. There were some disagreements between the measured  $T$  values and those calculated from theoretical equations.



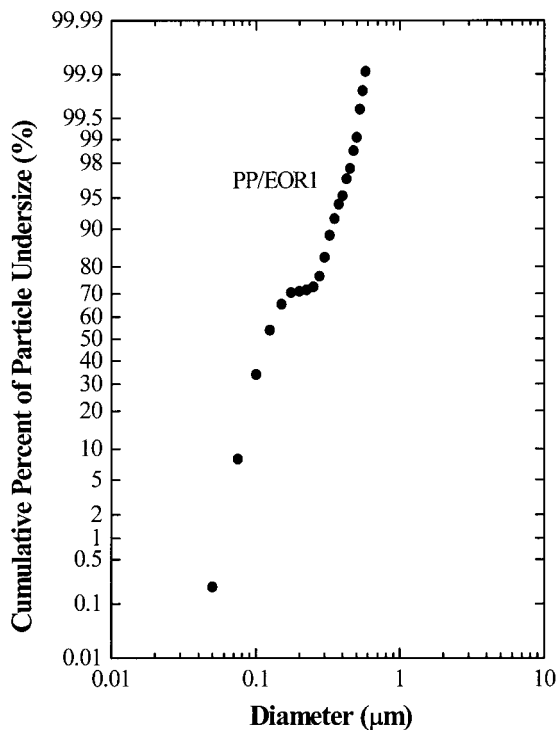


**Figure 6** Typical log-normal distributions of rubber particle sizes in PP/EOR1 blends.

We would like to thank Prof. T. Komoto, Assoc. Prof. T. Yamanobe, and Asst. Prof. H. Uehara of Gunma University for their suggestions with the characterization of EORs by GPC and NMR, and for helpful discussions.

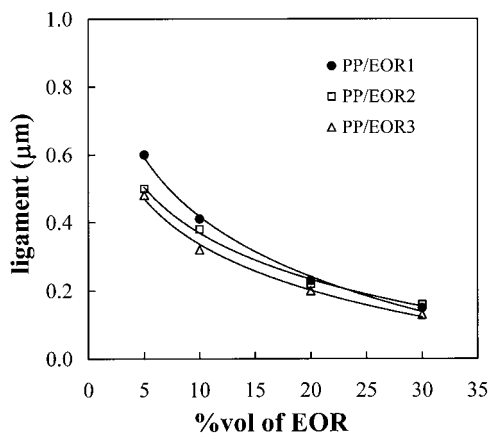


**Figure 7** Relationship between matrix ligament thickness and rubber concentration of PP/EOR1 ( $R^2 = 0.997$ ), PP/EOR2 ( $R^2 = 0.995$ ), and PP/EOR3 ( $R^2 = 0.994$ ) blends.

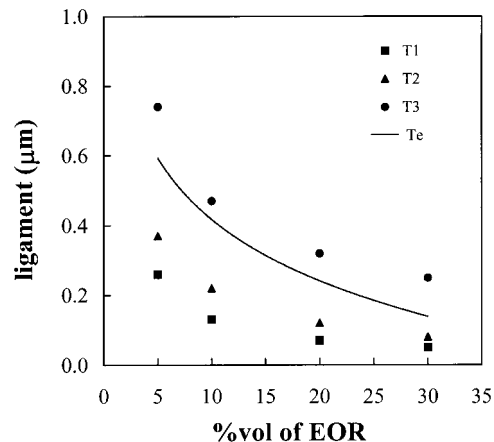


**Figure 8** Comparison of  $T$  values obtained from experimental measurement ( $T_e$ ) and theoretical calculations.  $T_1$ ,  $T_2$ , and  $T_3$  were calculated from eqs. (1), (2), and (3), respectively.

## REFERENCES

1. D'Orazio, L.; Mancarella, C.; Martuscelli, E.; Polato, F. *Polymer* 1991, 32, 1186.
2. Stehling, F. C.; Huff, T.; Speed, C. S.; Wissler, G. *J Appl Polym Sci* 1981, 26, 2693.
3. Karger-Kocsis, J.; Kallo, A.; Kuleznev, V. N. *Polymer* 1984, 25, 279.
4. van der Wal, A.; Nijhof, R.; Gaymans, R. J. *Polymer* 1999, 40, 6031.
5. Carriere, C. J.; Craig Silvis, H. *J Appl Polym Sci* 1997, 66, 1175.
6. Kukaleva, N.; Jollands, M.; Cser, F.; Kosior, E. *J Appl Polym Sci* 2000, 76, 1011.
7. Wu, S. *Polymer* 1985, 26, 1855.
8. Wu, S. *J Appl Polym Sci* 1988, 35, 549.
9. Gilbert, D.J.; Donald, A.M. *J Mater Sci* 1986, 21, 1819.
10. Borggreve, R. J. M.; Gayman, R. J.; Schuijjer, J. *Polymer* 1989, 30, 71.
11. Van der Sanden, M. C. M.; de Kok, J. M. M.; Meijer, H. E. H. *Polymer* 1994, 35, 2995.
12. Dijkstra, K.; ter Laak, J.; Gayman, R. J. *Polymer* 1994, 35, 315.
13. Jancar, J.; Dianselmo, A.; Dibenedetto, A. T. *Polym Commun* 1991, 32, 367.
14. Liu, Z. H.; Zhang, X. D.; Zhu, X. G.; Qi, Z. N.; Wang, F. S. *Polymer* 1997, 21, 5267.
15. Liu, Z. H.; Li, R. K. Y.; Tjong, S. C.; Qi, Z. N.; Wang, F. S.; Choy, C. L. *Polymer* 1998, 39, 4433.
16. Liu, Z. H.; Zhang, X. D.; Zhu, X. G.; Li, R. K. Y.; Qi, Z. N.; Wang, F. S.; Choy, C. L. *Polymer* 1998, 39, 5019.
17. Liu, Z. H.; Zhang, X. D.; Zhu, X. G.; Qi, Z. N.; Wang, F. S.; Li, R. K. Y.; Choy, C. L. *Polymer* 1998, 39, 5027.

18. Liu, Z. H.; Zhang, X. D.; Zhu, X. G.; Li, R. K. Y.; Qi, Z. N.; Wang, F. S.; Choy, C. L. *Polymer* 1998, 39, 5031.
19. Liu, Z. H.; Zhang, X. D.; Zhu, X. G.; Qi, Z. N.; Wang, F. S.; Li, R. K. Y.; Choy, C. L. *Polymer* 1998, 39, 5047.
20. Kim, H.; Keskkula, H.; Paul, D. R. *Polymer* 1990, 31, 869.
21. Majundar, B.; Keskkula, H.; Paul, D. R. *Polymer* 1994, 35, 3164.
22. Majundar, B.; Keskkula, H.; Paul, D. R. *Polymer* 1994, 35, 5453.
23. Majundar, B.; Keskkula, H.; Paul, D. R. *Polymer* 1994, 35, 5468.
24. Borggreve, R. J. M.; Gayman, R. J.; Schuijjer, J.; Ingen Housz, J. F. *Polymer* 1987, 28, 1489.
25. Irani, R. R.; Callis, C. F. *Particle size: Measurement, Interpretation and Application*; John Wiley & Sons: New York, 1963.
26. Denesi, S.; Porter, R. S. *Polymer* 1978, 19, 448.
27. Karger-Kocsis, J. K.; Csikai, I. *Polym Eng Sci* 1987, 27, 241.
28. Oshinski, A. J.; Keskkula, H.; Paul, D. R. *Polymer* 1996, 37, 4891.
29. Jang, B. Z.; Uhlmann, D. R.; Vander Sande, J. B. *Polym Eng Sci* 1985, 25, 643.
30. D'Orazio, L.; Mancarella, C.; Martuscelli, E.; Cecchin, G.; Corrieri, R. *Polymer* 1999, 40, 2745.
31. Favis, B. D.; Therrien, D. *Polymer* 1991, 32, 1474.
32. Burgisi, G.; Paternoster, M.; Peduto, N.; Saraceno, A. *J Appl Polym Sci* 1997, 66, 777.
33. Dharmarajan, N.; Kaufman, L. G. *Rubber Chem Technol* 1998, 71, 778.